OPEN

^{18}F-FACBC PET/MRI in Diagnostic Assessment and Neurosurgery of Gliomas

Anna Karlberg, MSc,† Erik Magnus Berntsen, MD, PhD,*† Håkon Johansen, MD,* Anne Jarstein Skjulsvik, MD,‡§ Ingerid Reinertsen, PhD,|| Hong Yan Dai, PhD,‡ Yiming Xiao, PhD,¶ Hassan Rivaz, PhD,**†† Per Borghammer, MD, PhD,‡‡ Ole Solheim, MD, PhD,§§|||¶¶ and Live Eikenes, PhD†*

Purpose: This pilot study aimed to evaluate the amino acid tracer ^{18}F-FACBC with simultaneous PET/MRI in diagnostic assessment and neurosurgery of gliomas.

Materials and Methods: Eleven patients with suspected primary or recurrent low- or high-grade glioma received an ^{18}F-FACBC PET/MRI examination before surgery. PET and MRI were used for diagnostic assessment, and for guiding tumor resection and histopathological tissue sampling. PET uptake, tumor-to-background ratios (TBRs), time-activity curves, as well as PET and MRI tumor volumes were evaluated. The sensitivities of lesion detection and to detect glioma tissue were calculated for PET, MRI, and combined PET/MRI with histopathology (biopsies for final diagnosis and additional image-localized biopsies) as reference.

Results: Overall sensitivity for lesion detection was 54.5% (95% confidence interval [CI], 23.4–83.3) for PET, 45.5% (95% CI, 16.7–76.6) for contrast-enhanced MRI (MRI_{CE}), and 100% (95% CI, 71.5–100.0) for combined PET/MRI, with a significant difference between MRI_{CE} and combined PET/MRI (P = 0.031). TBRs increased with tumor grade (P = 0.004) and were stable from 10 minutes post injection. PET tumor volumes enclosed most of the MRI_{CE} volumes (>98%) and were generally larger (1.5–2.8 times) than the MRI_{CE} volumes. Based on image-localized biopsies, combined PET/MRI demonstrated higher concurrence with malignant findings at histopathology (89.5%) than MRI_{CE} (26.3%).

Conclusions: Low- versus high-grade glioma differentiation may be possible with ^{18}F-FACBC using TBR. ^{18}F-FACBC PET/MRI outperformed MRI_{CE} in lesion detection and in detection of glioma tissue. More research is required to evaluate ^{18}F-FACBC properties, especially in grade II and III tumors, and for different subtypes of gliomas.

Key Words: PET/MRI, ^{18}F-FACBC, glioma, neurosurgery

(*Clin Nucl Med* 2019;44: 550–559)

Approximately one third of all primary brain tumors are malignant, and out of these, gliomas are the most common type accounting for almost 80%.[1,2] Although brain malignancy overall is relatively rare (the total incidence for gliomas is approximately 6 per 100,000 per year), these tumors cause significant mortality and morbidity.[3] Gliomas are classified according to World Health Organization (WHO) grades I to IV based on histopathological and molecular features,[4] and tumor grading is essential for the choice of therapies and for estimation of treatment response and overall prognosis.[5]

Routine examinations for patients with cerebral gliomas include histopathological tissue sampling and MRI. For primary diagnosis, histopathological evaluation is considered the criterion standard according to the recent 2016 WHO classification of tumors of the central nervous system.[4] However, due to the heterogeneous nature of gliomas, tissue sampling may result in sampling errors leading to underestimation of malignancy grade. Furthermore, MRI has limitations with respect to identifying tumor grade, true tumor extension, and differentiation of viable tumor tissue from treatment-induced changes and recurrences.

The introduction of clinically available PET/MRI systems in 2010[6] has resulted in new opportunities in advanced medical imaging procedures where anatomical, functional, and physiological images now can be acquired simultaneously with high diagnostic accuracy. PET/MRI has demonstrated great promise in areas where MRI is the predominant image modality, such as in neurological, cardiac, and soft tissue applications.[7–9] By combining the superior soft tissue contrast of MRI with the quantitative information of cellular activity and metabolism provided by PET, the diagnostic accuracy in glioma may likely improve.[10]

Amino acid (AA) PET is recommended by current guidelines as a complement to CT or MRI in brain tumor diagnostics, resection, biopsy, treatment planning, and therapy response assessment.[5,10,11] AA PET has also demonstrated additional value in noninvasive grading of gliomas by calculating the tracer uptake ratios or time-activity curves (TACs) from dynamic PET acquisitions.[12–14] However, the current recommendations for PET imaging in gliomas only cover the most widely used AA PET tracers (O-(2-[^{18}F] Fluoroethyl)-L-tyrosine [^{18}F-FET], L-[methyl-^{11}C]Methionine [^{11}C-MET], and L-3,4-Dihydroxy-6-[^{18}F]fluorophenylalanine [^{18}F-FDOPA]), whereas there are more than 20 additional AA PET tracers available for tumor imaging applications, including anti-1-amino-3-[^{18}F]fluorocyclobutane-1-carboxylic acid (^{18}F-FACBC),[15] also known as fluciclovine (^{18}F) or Axumin (Blue Earth Diagnostics

Received for publication January 23, 2019; revision accepted March 24, 2019.

From the *Department of Radiology and Nuclear Medicine, St Olavs Hospital; †Department of Circulation and Medical Imaging, Norwegian University of Science and Technology; ‡Department of Pathology and Medical Genetics, St Olavs Hospital; §Department of Laboratory Medicine, Children's and Women's Health, Faculty of Medicine, Norwegian University of Science and Technology; ||Department of Health Research, SINTEF, Trondheim, Norway; ¶Robarts Research Institute, Western University, London, Ontario, Canada; **PERFORM Centre, and ††Department of Electrical and Computer Engineering, Concordia University, Montreal, Quebec, Canada; ‡‡Department of Nuclear Medicine & PET Centre, Aarhus University Hospital, Aarhus, Denmark; §§Department of Neurosurgery, St Olavs Hospital; ||||Department of Neuroscience, Norwegian University of Science and Technology; and ¶¶Norwegian National Advisory Unit for Ultrasound and Image Guided Therapy, St Olavs Hospital, Trondheim, Norway.

Conflicts of interest and sources of funding: This work was supported by the Norwegian National Advisory Unit for Ultrasound and Image Guided Therapy, St Olavs Hospital, Trondheim, Norway. The authors report no conflicts of interest.

Correspondence to: Anna Karlberg, MSc, Department of Radiology and Nuclear Medicine, St Olavs Hospital, Olav Kyrres gt 17, N-7006 Trondheim, Norway. E-mail: annamka@stud.ntnu.no.

ISSN: 0363-9762/19/4407–0550
DOI: 10.1097/RLU.0000000000002610

Ltd, United Kingdom). ^{18}F-FACBC was originally developed for brain tumor applications,[16] but is most commonly used for prostate cancer imaging.[16–19] Only a few studies have evaluated the diagnostic performance of ^{18}F-FACBC in gliomas, suggesting benefits in the detection of glioma spread not detectable with contrast-enhanced MRI (MRI_{CE}).[20,21] Higher tumor-to-background ratios (TBRs) have also been found with ^{18}F-FACBC compared with the current recommended amino acid PET tracers,[21–24] implying that ^{18}F-FACBC may be superior for glioma detection compared with currently recommended tracers.

Differences in uptake and transport mechanisms may lead to variable uptake patterns among AA PET tracers. Nonnatural tracers, such as ^{18}F-FACBC, ^{18}F-FET, and ^{18}F-FDOPA, mainly represent transport, whereas the natural tracer ^{11}C-MET represents transport, protein synthesis, and nonprotein metabolic pathways.[15,25] Theoretically, this could indicate that dynamic analysis of ^{18}F-FACBC uptake could be useful in noninvasive grading of gliomas, as shown for ^{18}F-FET.[26–30] However, different AA transporter systems are involved for different AA PET tracers,[31] which may impact tracer distribution, including uptake in inflamed tissue, and blood-brain barrier (BBB) passage. Further studies of ^{18}F-FACBC are therefore needed to validate its potential in the workup of glioma patients.

The aim of this study was to assess the diagnostic value of ^{18}F-FACBC PET/MRI in patients with low- or high-grade glioma by analyzing and comparing PET uptake, tumor volumes, TBRs, and TACs to MRI and histopathology. Furthermore, the use of ^{18}F-FACBC PET/MRI in guiding surgical resection and tissue sampling was evaluated by comparing images to histopathology (image-localized biopsies).

MATERIALS AND METHODS

Subjects

Eleven patients (4 females) with suspected primary or recurrent low- or high-grade glioma were included in this study. Average patient age was 44 ± 18 years (range, 16–72 years). The patients received 3.11 ± 0.14 MBq/kg (average total dose, 235.5 ± 54.4 MBq) ^{18}F-FACBC at the onset of PET/MRI acquisition.

The study was approved by the Regional Ethics Committee (REK, reference number: 2016/279) and as a clinical trial of fluciclovine (^{18}F) by the Norwegian Medicines Agency (EudraCT no 2016–000939-41). All patients signed written informed consent to participate in the study.

Imaging

A hybrid PET/MRI system (Siemens Biograph mMR, Erlangen, Germany) was used for simultaneous PET and MRI acquisitions. Patients were injected with ^{18}F-FACBC on the examination table, and list-mode PET was acquired 0 to 45 minutes post injection (p.i.). MRI sequences were acquired according to current consensus recommendations on standardized brain tumor imaging protocols[32] and included pre– and post–contrast-enhanced 3D T1, 3D fluid attenuated inversion recovery (FLAIR), and T2, as well as an ultrashort echo time sequence for PET attenuation correction purposes. Diffusion, perfusion, and chemical shift imaging spectroscopy were also acquired, but were not analyzed in the current study.

PET Reconstruction and Analysis

PET image reconstruction was performed with iterative reconstruction (3D OSEM algorithm, 3 iterations, 21 subsets, 344 × 344 matrix, 4-mm Gaussian filter) with point spread function, decay, scatter, and attenuation correction. Static PET images (30–45 minutes p.i.) were used for calculations of SUVs based on patient body weight and estimation of TBRs. A volume of interest (VOI) covering the whole tumor was placed manually on the reconstructed static PET images (defined by FLAIR for PET-negative tumors; PMOD software version 3.903; PMOD Technologies LLC, Zürich, Switzerland) to assess the highest tumor uptake (SUV_{max}). SUV_{peak} was defined semiautomatically by letting the program select a spherical peak VOI (2 mL) covering the region with highest activity uptake to assess the average uptake in a larger region of the tumor. The mean background uptake (SUV_{bg}) was calculated by placing a VOI (2 mL) in the contralateral hemisphere, avoiding the ventricles. TBR_{max} and TBR_{peak} were calculated as tumor SUV_{max} and SUV_{peak} divided by SUV_{bg}.

For estimation of TACs and TBR dependence over time, list-mode PET data were reconstructed into 12 × 5-, 6 × 10-, 6 × 30-, 5 × 60-, and 7 × 300-second frames. PMOD was used for dynamic analysis of PET data. TBR_{peak} variations over time were calculated for PET-positive tumors by dividing SUV_{peak} by SUV_{bg} for each time point.

Clinical Evaluation of PET and MRI Scans

A nuclear medicine physician evaluated the static PET images, and a neuroradiologist evaluated the MRI scans. In this cohort of patients, tumors with TBR_{peak} greater than 2 were classified as PET positive.

Pathology on MRI scans was assessed and defined by contrast enhancement on T1, high-intensity on T2 and FLAIR (excluding edema), and/or low-intensity on precontrast T1 (see Tumor Volume Delineation). The overall assessment of MRI was based on all MRI sequences (FLAIR, T1, and T2) and denoted MRI*.

Tumor Volume Delineation

Tumor volumes were defined for PET, high-intensity FLAIR ($FLAIR_{HI}$), MRI_{CE}, and for the overall estimated MRI tumor volume (MRI_{Tumor}; based on FLAIR, T1, and T2) using PMOD.

The PET tumor volumes were delineated by applying a large continuous search VOI covering the whole tumor and subsequently applying an isocontour at $2xSUV_{bg}$ for voxels within the VOI. Regions considered to be nontumor tissue (ie, vessels and meningea) inside the segmented volume were excluded manually, and the final PET tumor volume was calculated.

$FLAIR_{HI}$ and MRI_{CE} tumor volumes were delineated using a large VOI covering the whole tumor and subsequently applying a manually adjusted threshold value to fit the visual volume as judged by the neuroradiologist. $FLAIR_{HI}$ occasionally also include peritumoral edema, and parts of the FLAIR images deemed as edema were manually removed by an experienced neuroradiologist, to assess MRI_{Tumor}, using T1 and T2 as guidance.

All volume estimations were performed with matched PET and MRI datasets, where PET was registered to the MRI. The intersected PET and MRI (MRI_{CE}, $FLAIR_{HI}$, and MRI_{Tumor}) volumes were calculated as the percentage of the different MRI volumes enclosed in the PET volume of each patient.

Histopathological Tissue Sampling and Surgery

Static PET images were fused with FLAIR images (and T1 postcontrast for tumors with contrast enhancement) and imported into the Sonowand Invite Neuronavigation System (Sonowand AS, Trondheim, Norway) together with FLAIR and contrast-enhanced T1 before surgery. These images were used together with intraoperative 3D ultrasound during histopathological tissue sampling and resection.[33] One large (nonlocalized) biopsy was extracted from the central parts of each tumor before resection. The large biopsy was used for the final histopathological diagnosis. Five patients gave written consent to the Mid-Norway Brain Tumor

Registry and Biobank to collect 3 to 4 image-localized biopsies from their tumors for histopathological analysis, and these were taken from different regions in the tumor before resection. The biopsies were diagnosed according to the current WHO classification with *IDH1 R132H* mutation, 1p/19q codeletion, *TP53* mutation, and *ATRX* mutation. MGMT promoter methylation, TERT promotor mutation, and Ki67 labeling index were also obtained. Full descriptions of histopathological tissue sampling, analyses, and surgery were published previously.[34] To accurately localize the biopsies in the PET/MRI scans and to recover brain shift, the intraoperative 3D ultrasound was nonlinearly registered to the presurgical FLAIR after surgery using RaPTOR (robust patch-based correlation ratio) algorithm in MATLAB.[35] The coordinates were then transposed to PET and MRI scans in PMOD to correlate the histopathological results with the image results for each biopsy.

Statistical Analysis

The overall sensitivity of lesion detection was calculated for PET, MRI_{CE}, and combined PET/MRI* using the large nonlocalized biopsies/final histopathological diagnosis as reference for all patients (only imaging as reference for patient 9). McNemar exact test for correlated proportions was used for statistical comparison of MRI_{CE} to PET/MRI* and of PET to MRI_{CE}; $P \leq 0.05$ was considered statistically significant. The 95% confidence intervals (CIs) were calculated using the Clopper-Pearson exact method and Stata/MP (version 15.1; StataCorp LLC, College Station, TX). To compare ^{18}F-FACBC uptake (TBR_{max}, TBR_{mean}, SUV_{max}, and SUV_{mean}) between tumor grades (II, III, and IV), a Kruskal-Wallis test was applied (using IBM SPSS Statistics 25), and $P \leq 0.05$ was considered statistically significant.

The sensitivity to detect glioma tissue was calculated by comparing PET, MRI_{CE}, $FLAIR_{HI}$, MRI_{Tumor}, and PET/MRI_{Tumor} to histopathological results based on the image-localized biopsies taken from 5 patients before resection. Because the sample size of the data was small and there were dependencies in the data (3–4 biopsies/patient), no statistical comparisons were performed for the detection of glioma tissue.

RESULTS

Clinical Evaluation

Histopathology revealed 5 grade IV tumors (glioblastoma), 2 grade III tumors (1 anaplastic oligodendroglioma and 1 anaplastic astrocytoma), and 3 grade II tumors (2 oligodendrogliomas, 1 diffuse astrocytoma; Table 1). In one tumor, tissue sampling was unobtainable due to localization in the brainstem, and this tumor was diagnosed as a low-grade glioma (grade II) based on MRI findings. Six of the patients demonstrated tumor uptake of ^{18}F-FACBC and were considered PET positive by the nuclear medicine physician (all grade IV and 1 grade III; Table 1 and Fig. 1). TBR was higher for the high-grade tumors compared with the low-grade tumors. The background activity was generally low, with an average of $SUV_{bg} = 0.36 \pm 0.14$. On MRI, all tumors were considered pathological based on FLAIR, T1 (precontrast and postcontrast), and T2 images by the neuroradiologist. However, only grade IV tumors showed contrast enhancement.

The overall sensitivity of lesion detection (Table 1) was 54.5% (95% CI, 23.4–83.3) for PET, 45.5% (95% CI, 16.7–76.6) for MRI_{CE}, and 100% (95% CI, 71.5–100.0) for combined PET/MRI* (including all MRI scans; FLAIR, T1, and T2). There was a significant difference in lesion detection between MRI_{CE} and combined PET/MRI* ($P = 0.031$), but not between MRI_{CE} and PET ($P = 1.000$).

^{18}F-FACBC uptake increased with tumor grade, and significant differences in tumor uptake between grades were observed ($P = 0.004$ for TBR_{max} and TBR_{mean}, $P = 0.007$ for SUV_{max}, and $P = 0.015$ for SUV_{mean}).

Dynamic PET Analysis

The mean tumor uptake over time (SUV_{max}) for PET-positive tumors reached a peak at 43 seconds p.i., and after stabilization, a slow increase was observed. SUV_{peak} did not reach maximum during the 45 minutes acquisition but was continuously increasing from 5 minutes p.i.. Activity uptake in normal brain (SUV_{bg}) showed a slow increase from 2 minutes p.i. (Fig. 2A). TBR_{peak} was found to be stable from 10 minutes p.i. (Fig. 2B).

TABLE 1. Summary of All Patients and Clinical Evaluations

Patient	Age	Sex	Primary/ Recurrent Tumor	Histopathological Diagnosis (WHO Grade)	TBR_{max}/SUV_{max}	TBR_{peak}/SUV_{peak}	SUV_{bg}	PET	MRI_{CE}	PET/MRI*
2	55	M	Recurrence	Glioblastoma (IV)	24.6/5.5	14.3/3.2	0.2	Yes	Yes	Yes
7	57	M	Primary	Glioblastoma (IV)	20.0/6.9	9.2/3.2	0.4	Yes	Yes	Yes
4	72	M	Primary	Glioblastoma (IV)	14.5/4.6	8.0/2.5	0.3	Yes	Yes	Yes
10	59	F	Recurrence	Glioblastoma (IV)	10.1/7.3	6.5/4.7	0.7	Yes	Yes	Yes
11†	16	M	Primary	Glioblastoma (IV)	8.2/1.8	6.0/1.3	0.2	Yes	Yes	Yes
1	60	F	Primary	Anaplastic oligodendroglioma (III)	4.2/1.8	3.2/1.4	0.4	Yes	No	Yes
3	42	M	Recurrence	Oligodendroglioma (II)	3.9/1.5‡	2.0/0.8‡	0.4	No	No	Yes
6	21	M	Primary	Oligodendroglioma (II)	3.5/1.0‡	1.6/0.4‡	0.3	No	No	Yes
8	40	F	Primary	Anaplastic astrocytoma (III)	3.0/1.0‡	1.1/0.4‡	0.4	No	No	Yes
9	36	F	Primary	Low-grade glioma (II)§	1.4/0.5	1.1/0.4	0.4	No	No	Yes
5	26	M	Primary	Diffuse astrocytoma (II)	1.4/0.4	1.0/0.3	0.3	No	No	Yes

All patients included in the study with final histopathological diagnosis, SUV (max, peak, and background), TBR (max and peak), and clinical PET and MRI results. Pathological results are denoted "yes" and nonpathological results are denoted "no." The patients are ordered from highest to lowest TBR.

*Overall assessment based on FLAIR, T1, and T2 images.

†PET image acquisition was interrupted due to anxious patient and images were therefore reconstructed 45–60 minutes post injection.

‡Higher values were found in these tumors due to spill-out effects from tissue with higher uptake and were considered PET negative by nuclear medicine physician.

§No biopsy possible due to tumor location in brain stem.

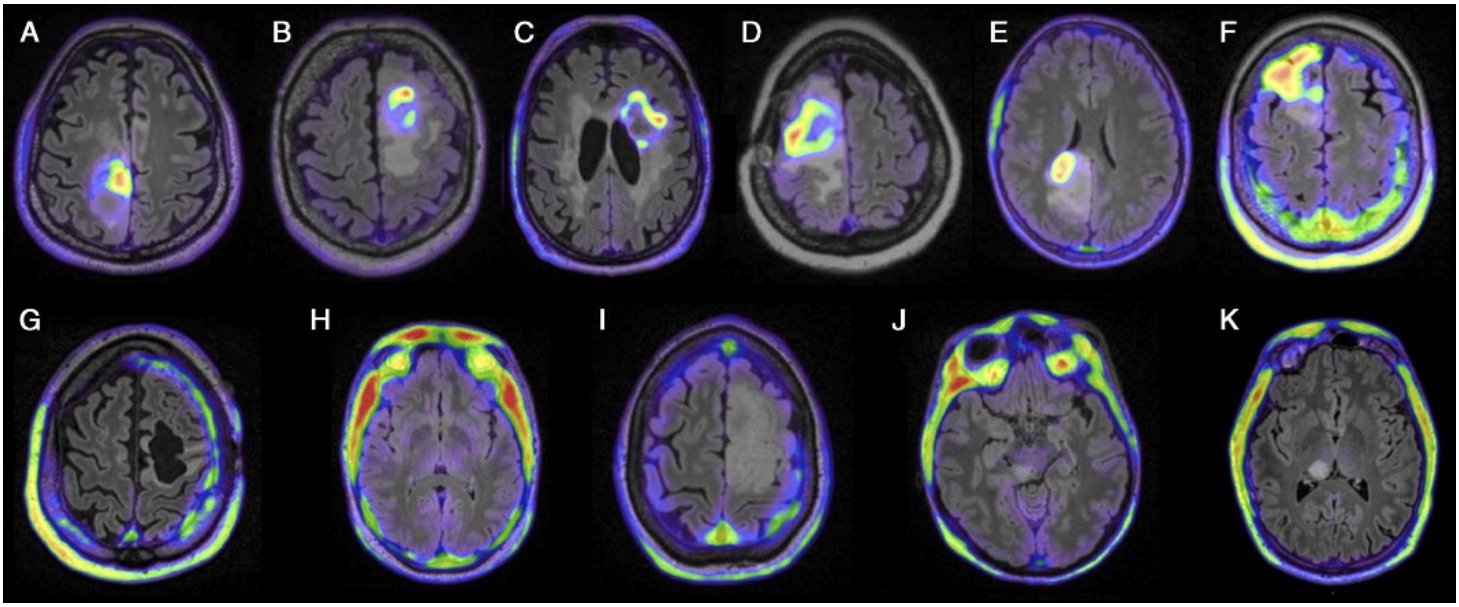

FIGURE 1. Fused PET/FLAIR images of all patients ordered from highest to lowest TBR. Patients with PET-positive tumors in top row: (**A**) patient 2, (**B**) patient 7, (**C**) patient 4, (**D**) patient 10, (**E**) patient 11, and (**F**) patient 1. Patients with PET-negative tumors in bottom row: (**G**) patient 3, (**H**) patient 6, (**I**) patient 8, (**J**) patient 9, and (**K**) patient 5. The PET color scale was set from SUV_{bg} to SUV_{max} for PET-positive tumors and from SUV_{bg} to SUV = 2 for PET-negative tumors, to better visualize the MRI scans.

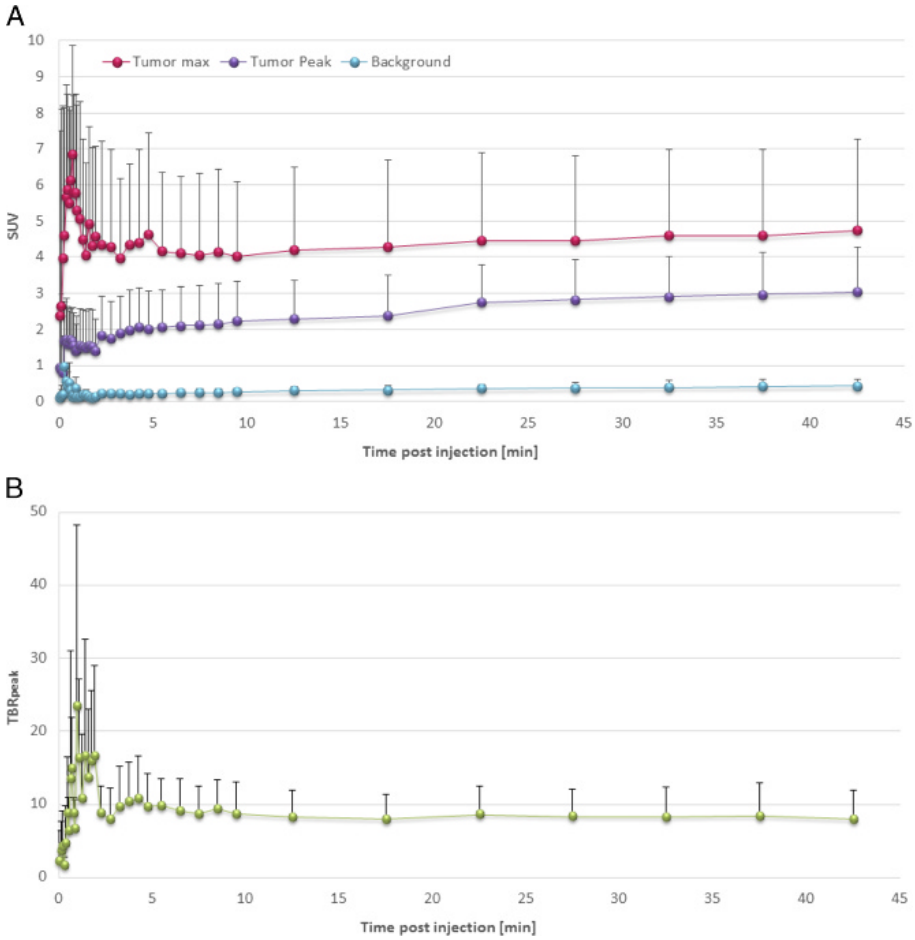

FIGURE 2. **A**, Tumor maximum (SUV_{max}), tumor peak (SUV_{peak}), and background uptake (SUV_{bg}). **B**, Peak tumor-to-background ratio (TBR_{peak}) with time for the PET-positive tumors (patients 1, 2, 4, 7, 10, and 11). Standard deviations are given for each time point. The large standard deviation in TBR_{peak} at 1 minute was due to movement of 1 patient.

TABLE 2. Tumor Volumes

Patient	PET, cm^3	MRI_{CE}, cm^3	$FLAIR_{HI}$, cm^3	MRI_{Tumor}, cm^3	Intersect PET and MRI_{CE}, %	Intersect PET and $FLAIR_{HI}$, %	Intersect PET and MRI_{Tumor}, %
2	68.8*	26.6*	62.8†	52.5*	100	78.6	91.4
7	18.9	9.9	58.7‡	9.9§	98.3	27.1	98.3
4	45.0	22.3	NA‖	NA‖	99.7	NA‖	NA‖
10	28.0	18.4	85.2‡	18.4§	98.9	29.9	98.9
11	9.6	3.4	76.1	76.1	99.7	11.2	11.2
1	16.7	—	23.6	23.6	—	56.4	56.4
3	—	—	9.1	7.2	—	—	—
6	—	—	2.6	2.6	—	—	—
8	—	—	44.2	44.2	—	—	—
9	—	—	0.7	0.7	—	—	—
5	—	—	2.1	2.1	—	—	—

Tumor volumes as defined for PET, MRI_{CE}, $FLAIR_{HI}$, and MRI_{Tumor}. The intersected PET and MRI (MRI_{CE}, $FLAIR_{HI}$, and MRI_{Tumor}) volumes were calculated as the percentage of the different MRI volumes enclosed in the PET volume of each patient. The patients are ordered from highest to lowest TBR.

*Including surgical cavity.

†Including edema, white matter changes, and surgical cavity.

‡Tumor surrounded by edema.

§Tumor component on FLAIR images is equal to contrast-enhanced MRI region as judged by an experienced neuroradiologist.

‖Not applicable. Not possible to differentiate tumor tissue from confluent white matter changes (Fazekas grade 3).

Tumor Volumes

Tumor volumes defined by PET enclosed most of the MRI_{CE} volume (intersection >98%) and were larger (1.5–2.8 times the MRI_{CE} volume) for the PET-positive tumors. The $FLAIR_{HI}$ volumes were generally larger than the PET volumes, whereas the MRI_{Tumor} volumes varied in size compared with the PET volume (Table 2 and Fig. 3).

Image-Localized Biopsies

Nineteen image-localized biopsies were extracted from 5 patients. The biopsy sites, overlaid on PET/FLAIR images, are shown in Figure 4. The corresponding histopathological, PET, and MRI results are summarized in Table 3. PET was positive for all grade IV samples, for 8 of 14 grade II/III samples, and for 1 of 2 grade II samples; however, all samples associated with anaplastic astrocytoma were PET negative.

The observed sensitivity to detect glioma tissue, based on image-localized biopsies (Table 3), was 63.2% for PET, 26.3% for MRI_{CE}, 100% for $FLAIR_{HI}$, and 73.7% for MRI_{Tumor}. Combined PET/MRI_{Tumor} had higher sensitivity (89.5%) than PET or MRI_{Tumor} alone.

Cell proliferation (Ki67 labeling index) were generally higher for PET-positive samples with mean Ki67 of 6.7% for PET-positive samples and mean Ki67 of 3.9% for PET-negative samples. Six of

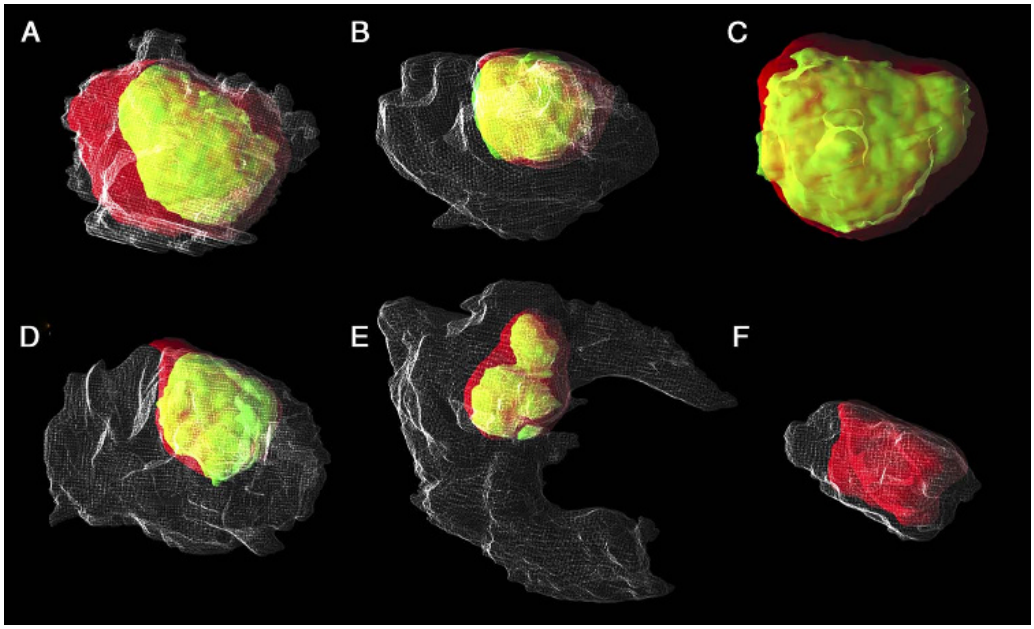

FIGURE 3. Tumor volumes defined by PET (red), $FLAIR_{HI}$ (gray), and MRI_{CE} (green) for patients with PET-positive tumors ordered from highest to lowest TBR. Grade IV tumors: (**A**) patient 2, (**B**) patient 7, (**C**) patient 4, (**D**) patient 10, and (**E**) patient 11, and the grade III tumor: (**F**) patient 1.

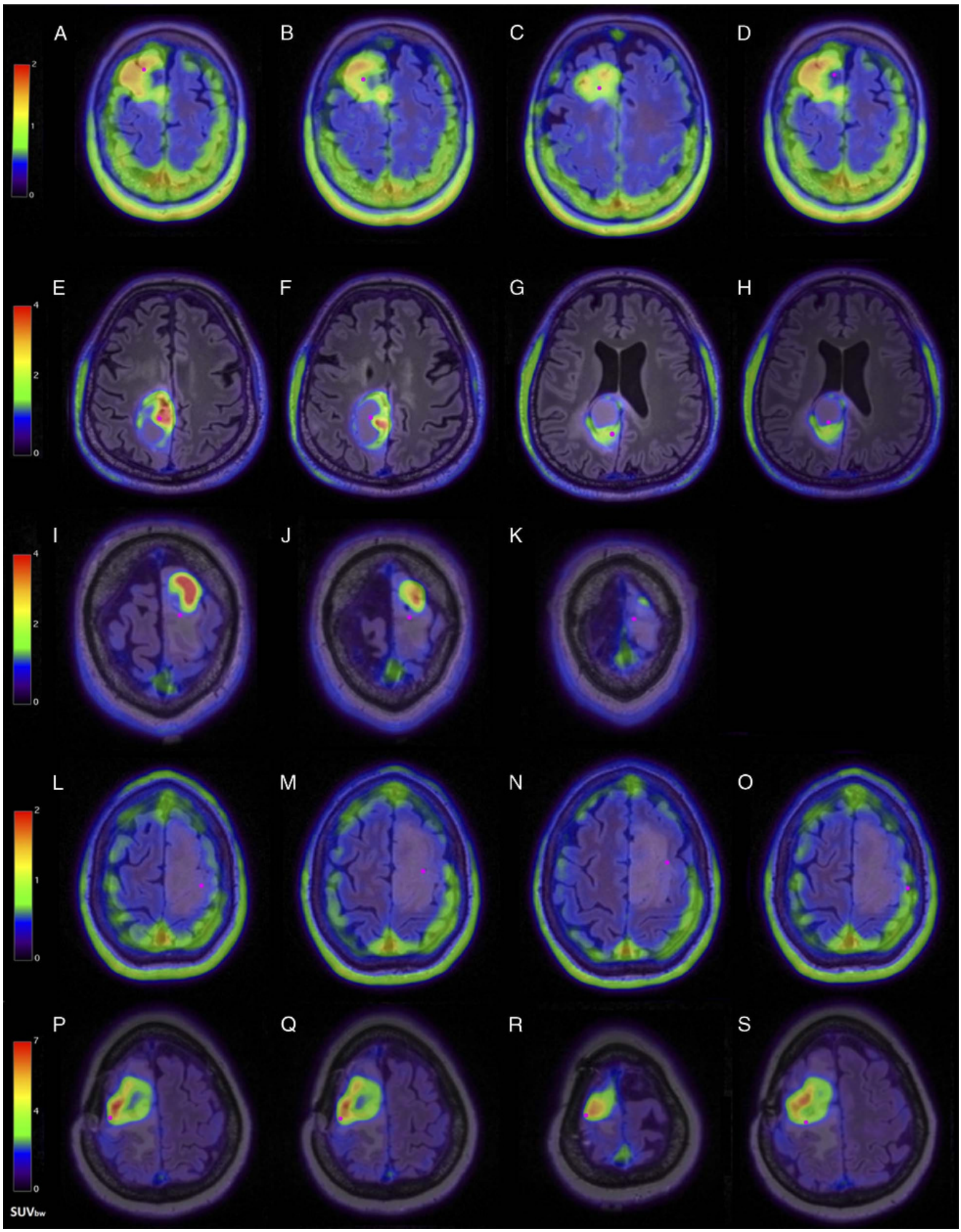

FIGURE 4. Fused PET/FLAIR images with localized biopsy sites (marked in pink) for (**A**–**D**) patient 1, (**E**–**H**) patient 2, (**I**–**K**) patient 7, (**L**–**O**) patient 8, and (**P**–**S**) patient 10.

TABLE 3. Results for the Image-Localized Biopsies

Patient	Biopsy	Histopathologic Diagnosis (WHO Grade, Ki67, Cell Density, Tumor Markers Present)	PET	MRI_{CE}	$FLAIR_{HI}$	MRI_{Tumor}	PET/MRI_{Tumor}
1	Nonlocalized biopsy*	Anaplastic oligodendroglioma (III, 20%, high, *IDH1 R132H*, 1p/19q, MGMT, TERT)					
	A	II/III, 12%, high, *IDH1 R132H*, 1p/19q, TERT	1.6 (+)	−	+	+	+
	B	II/III, 8%, high, *IDH1 R132H*, 1p/19q, TERT	0.9 (+)	−	+	+	+
	C	II, 8%, moderate, *IDH1 R132H*, 1p/19q, TERT	1.0 (+)	−	+	+	+
	D*	II, 5%, moderate, *IDH1 R132H*, 1p/19q	0.5 (−)	−	+	+	+
2	Nonlocalized biopsy	Glioblastoma (IV, 20%, high, TP53)					
	E	III, 9%, moderate	4.7 (+)	+	+	+	+
	F	IV, 10%, high	1.2 (+)	+‡	+	+	+
	G†	III, 9%, high	1.6 (+)	−	+	+	+
	H	III, 9%, high	0.7 (+)	+‡	+	+	+
7	Nonlocalized biopsy	Glioblastoma (IV, 20%, high, MGMT, TERT)					
	I	II/III, 1%, moderate, MGMT, TERT	0.7 (+)	+	+	+	+
	J	III, 15%, high, MGMT, TERT	0.5 (−)	−	+	−	−
	K	II/III, 1%, moderate, MGMT, TERT	0.8 (−)	−	+	−	−
8	Nonlocalized biopsy	Anaplastic astrocytoma (III, 11%, high, *IDH1 R132H*, TP53, ATRX)					
	L	III, 2%, moderate, ATRX	0.3 (−)	−	+	+	+
	M†	II/III, 1%, moderate, ATRX	0.3 (−)	−	+	+	+
	N	III, 1%, moderate, *IDH1 R132H*, ATRX	0.3 (−)	−	+	+	+
	O	III, 2%, moderate, ATRX	0.6 (−)	−	+	+	+
10	Nonlocalized biopsy	Glioblastoma (IV, 24%, high)					
	P*†	III, 1%, moderate	4.0 (+)	−§	+	−	+
	Q	III, 2%, moderate	4.1 (+)	−§	+	−	+
	R	IV, 6%, high	4.4 (+)	−§	+	−	+
	S	IV, 5%, high	3.0 (+)	+	+	+	+

Histopathological, PET, and MRI results of the patients (1, 2, 7, 8, and 10) where image-localized biopsies were sampled.

*Inconclusive for MGMT promoter methylation due to small amount of tissue or small amount of degraded DNA.

†Inconclusive for TERT promoter mutation due to small amount of tissue or small amount of degraded DNA.

‡Positive, but in necrotic area.

§Negative, but close to MRI_{CE} region.

7 samples with high cell density were PET positive. Four of 6 samples expressing TERT promoter methylation, 3 of 5 samples expressing *IDH1 R132H*, 3 of 4 samples expressing 1p/19q codeletion, and 1 of 3 samples expressing MGMT promoter methylation were PET positive. Samples with *ATRX* mutation were PET negative. None of the image-localized biopsies expressed *TP53* mutation.

Nonlocalized Biopsies

Full histopathological results for the nonlocalized biopsies in 5 of the patients is found in Table 3. PET was positive in tumors expressing MGMT promoter methylation, TERT promoter mutation, and/or 1p/19q codeletion. PET was negative in the tumor expressing *ATRX* mutation. Tumors expressing *IDH1 R132H* and/or *TP53* mutation were either PET positive or PET negative.

DISCUSSION

This is one of the first studies evaluating the amino acid PET tracer ^{18}F-FACBC in patients with suspected primary or recurrent low- or high-grade glioma and, to our knowledge, the first study to use simultaneous ^{18}F-FACBC PET/MRI in diagnostic assessment and neurosurgery of gliomas.

^{18}F-FACBC uptake in high-grade tumors was generally high, whereas uptake in normal brain was low, resulting in higher TBR compared with other amino acids used in brain tumor imaging, but comparable to other studies using ^{18}F-FACBC in glioma evaluation. This indicates that ^{18}F-FACBC could be better suited for high-grade glioma detection than, for example, ^{11}C-MET, especially for very small tumors.[21–24] Of interest, our data suggest that ^{18}F-FACBC tumor uptake alone may be sufficient to differentiate low- from high-grade gliomas with reasonable accuracy, because significant differences in tumor uptake (TBR and SUV) between grades were found. However, this assertion needs to be studied in larger samples of well-characterized gliomas.

All glioblastomas and anaplastic oligodendrogliomas showed ^{18}F-FACBC uptake in our study as well as in previous studies.[20,21,24] However, there are reported uptake differences for grade II and III tumors using ^{18}F-FACBC. For other AA PET tracers, approximately two thirds of low-grade gliomas show tracer uptake,[36] but in our study, no PET uptake was observed in all 4 grade II tumors and in 1 grade III (anaplastic astrocytoma) tumor. Another study evaluating the same PET tracer in low- and high-grade tumors found PET uptake in all tumors, including grade II diffuse astrocytomas.[24] However, in that study, 2 diffuse astrocytomas demonstrated a lesion-to-contralateral normal brain tissue (L/N) ratio less than 2, which would have been considered PET negative in our study. Furthermore, 1 grade II oligodendroglioma and 1 grade III anaplastic astrocytoma were clearly PET positive in their study,

whereas these type of tumors were PET negative in our study. Wakabayashi et al[20] compared histopathology (35 patients, 46 biopsy specimens) with ^{18}F-FACBC uptake in low- and high-grade gliomas, and reported uptake in most low-grade tumors/specimens. However, the criterion for PET positivity was not stated in that study, and comparison to our results is therefore difficult. Commonly used TBR thresholds for defining biological tumor volumes (ie, PET-positive regions) for other AA PET tracers vary between 1.3 and 2.0 for ^{11}C-MET, ^{18}F-FET, and ^{18}F-FDOPA.[37–39] In this study, a TBR of 2.0 was chosen ($2xSUV_{bg}$), but the optimal TBR cutoff for ^{18}F-FACBC needs further validation in future studies.

For all PET-positive tumors, the uptake pattern appeared quite similar to the results of Kondo et al[21] with rather stable TACs until the end of acquisition. The dynamic uptake demonstrated that the TBR was constant 10 to 45 minutes p.i., which indicates that static PET acquisitions should preferably be performed within this interval.

Of interest, there seems to be differences in the tumor tracer kinetics between ^{18}F-FACBC and ^{18}F-FET. The continuously increasing TAC, typical for low-grade tumors, and decreasing TAC, typical for high-grade tumors with ^{18}F-FET,[26–30] cannot be robustly evaluated with ^{18}F-FACBC due to the very low uptake in low-grade tumors.[24] A possible explanation for the apparent differences between the dynamic properties of ^{18}F-FACBC and ^{18}F-FET could be the different transport mechanisms involved in AA transport. For ^{18}F-FET, the uptake in cancer cells is primarily regulated by leucine preferring system L,[15,40] and the L-type amino acid transporter 1 (LAT1) has been proven to be responsible for the intracellular accumulation of ^{18}F-FET in glioma cell lines.[41,42] ^{18}F-FACBC uptake is mediated by both LAT1 and alanine-serine-cysteine transporter 2 (ASCT2), but with higher affinity for the latter.[43–45] Both LAT1 and ASCT2 are substantially upregulated in many cancerous tissues relative to most other AA transporters.[46] LAT1 expression correlates with cell proliferation and angiogenesis.[47] ASCT2 seems to have an important role in tumor progression, because the expression is elevated in human cancer cells such as hepatocellular carcinoma, colorectal cancer, breast cancer, prostate cancer, and gliomas.[15,48] ASCT2 expression has been shown to be ~2.5-fold higher in anaplastic astrocytoma tissue, glioblastoma tissue, glioma cultures, and metastases compared with control tissue.[49] System L AA transport system is advantageous in brain tumor imaging due to the ability to cross the BBB,[31] and it seems possible that the difference between PET uptake of ^{18}F-FACBC and other AAs could be due to different roles of the AA transporter mechanisms at the BBB. Another possible explanation could be different intracellular fates of the AAs after transport to the tumor tissue. Our results indicate that dynamic ^{18}F-FET PET is preferable over dynamic ^{18}F-FACBC PET to differentiate between glioma grades and types.

The PET volumes were larger than the MRI_{CE} volumes and enclosed most MRI_{CE} volumes almost completely. This corresponds well to previous studies demonstrating that PET was able to detect glioma spread that was not detectable by MRI_{CE}.[20,21] For patient 1 (anaplastic oligodendroglioma), no contrast enhancement was detected, whereas a clear PET uptake was observed. This could indicate that the tumor underwent recent malignant transformation better detected by ^{18}F-FACBC PET than MRI_{CE}. Unterrainer et al[50] demonstrated that ^{18}F-FET PET showed a high detection rate of both tumor progression and malignant transformations, even before progression on MRI was observed, and it is possible that the same is true for ^{18}F-FACBC. The $FLAIR_{HI}$ volume was generally larger than the PET volume, but it was clearly difficult to delineate the biological tumor volume based on $FLAIR_{HI}$, T1, and T2 (here MRI_{Tumor}) for grade IV tumors. It was a highly subjective approach, and although the sensitivity for MRI_{Tumor} was higher (73.7%) than for PET (63.2%), adding PET to the MRI examination will increase the sensitivity to detect glioma tissue up to 89.5%. Using $FLAIR_{HI}$ alone to detect tumor tissue could be tempting given the sensitivity shown in this study, but one has to consider that all the biopsies were collected closely to the main tumor bulk and not in the periphery, thus overestimating the sensitivity of $FLAIR_{HI}$. It is well known that other conditions involving white matter gives an increased FLAIR signal, such as vasogenic edema.[51]

A thorough analysis of each image-localized biopsy was performed to evaluate whether ^{18}F-FACBC PET uptake was related to specific tumor properties and markers. PET-positive samples had generally higher tumor grade, Ki67 labeling index, and cell density, in accordance with previous studies.[20,34] LAT1 expression correlates with cell proliferation,[47] which may explain the higher Ki67 values for PET-positive samples. The majority of the samples expressing 1p/19q codeletion and TERT promoter mutation were PET positive. Furthermore, tumors expressing 1p/19q codeletion, TERT promoter mutation, and/or MGMT promoter methylation were PET positive, which could indicate an association between these tumor markers and PET uptake. In support, Tsuyuguchi et al[24] found an association between TERT promoter mutation and high PET uptake. Of note, both TERT promoter mutation and MGMT promoter methylation have been shown to predict prognosis in patients with glioblastoma.[52] However, the relation between these tumor markers and ^{18}F-FACBC uptake should be evaluated further in larger studies.

This pilot study has several limitations, of which the small sample size can be considered one of the most important. Furthermore, image-localized biopsies should have been sampled also from regions without tumor components, but this was not performed in the current study due to the extra risk associated with such procedures in the brain. This is a major drawback in the context of proper statistical analyses, because specificity, accuracy, and negative predictive values become inconsiderable, and all positive predictive values become 100%.

PET/MRI scan registration to the intraoperative 3D ultrasound is another limitation. The error associated with the RaPTOR registration algorithm is estimated to be ~1 to 2 mm.[53] Some samples were taken close to the border of PET and MRI_{CE} regions according to the performed registration, and these samples may have been vulnerable to this registration error. Tumor shift is another limitation, which may have led to some biopsies not being sampled from the desired place due to suboptimal insight. Our sampling method did not contain automatic, intraoperative brain shift compensation.

CONCLUSIONS

TBRs were higher for ^{18}F-FACBC compared with other tracers for brain tumor imaging, and tumor uptake increased with tumor grade, indicating that low- versus high-grade glioma differentiation may be possible using the uptake levels of the tumors. In contrast, the potential for differentiating tumor grades by means of TAC characteristics is limited due to low tracer uptake in low-grade tumors. ^{18}F-FACBC PET/MRI delineated tumor extension better than MRI_{CE} and outperformed MRI_{CE} in detection of glioma tissue. ^{18}F-FACBC PET is suitable for histopathological tissue sampling and tumor resection, because tumor grade, cell proliferation, and cell density in PET-positive regions were found to be high. Further studies are needed to evaluate ^{18}F-FACBC properties, especially in grade II and III tumors.

ACKNOWLEDGMENTS

The authors would like to thank Lisa Millgård Sagberg and Camilla Brattbakk at the Department of Neurosurgery at St Olavs Hospital,

Trondheim, Norway, for their valuable assistance in providing clinical and specimen information. We would also like to thank Pål Sørensen, at the same department, for his assistance with image transfers to the neuronavigation system. Thanks also to Turid Follestad, Associate Professor in Medical Statistics, Unit of Applied Clinical Research, Faculty of Medicine and Health Sciences, Norwegian University of Science and Technology, Trondheim, Norway, for the useful discussions and verification of statistical calculations.

REFERENCES

1. Ostrom QT, Gittleman H, Fulop J, et al. CBTRUS Statistical Report: Primary Brain and Central Nervous System Tumors Diagnosed in the United States in 2008–2012. *Neuro Oncol*. 2015;17:iv1–iv62.
2. Schwartzbaum JA, Fisher JL, Aldape KD, et al. Epidemiology and molecular pathology of glioma. *Nat Clin Pract Neurol*. 2006;2:494–503.
3. Ho VK, Reijneveld JC, Enting RH, et al. Changing incidence and improved survival of gliomas. *Eur J Cancer*. 2014;50:2309–2318.
4. Louis DN, Perry A, Reifenberger G, et al. The 2016 World Health Organization Classification of Tumors of the Central Nervous System: a summary. *Acta Neuropathol*. 2016;131:803–820.
5. Vander Borght T, Asenbaum S, Bartenstein P, et al. EANM procedure guidelines for brain tumour imaging using labelled amino acid analogues. *Eur J Nucl Med Mol Imaging*. 2006;33:1374–1380.
6. Muzic RF Jr, DiFilippo FP. Positron emission tomography–magnetic resonance imaging: technical review. *Semin Roentgenol*. 2014;49:242–254.
7. Miller-Thomas MM, Benzinger TL. Neurologic applications of PET/MR imaging. *Magn Reson Imaging Clin N Am*. 2017;25:297–313.
8. Lau JM, Laforest R, Nensa F, et al. Cardiac applications of PET/MR imaging. *Magn Reson Imaging Clin N Am*. 2017;25:325–333.
9. Fraum TJ, Fowler KJ, McConathy J. PET/MRI: emerging clinical applications in oncology. *Acad Radiol*. 2016;23:220–236.
10. Albert NL, Weller M, Suchorska B, et al. Response assessment in Neuro-Oncology Working Group and European Association for Neuro-Oncology recommendations for the clinical use of PET imaging in gliomas. *Neuro Oncol*. 2016;18:1199–1208.
11. Law I, Albert NL, Arbizu J, et al. Joint EANM/EANO/RANO practice guidelines/SNMMI procedure standards for imaging of gliomas using PET with radiolabelled amino acids and [(18)F]FDG: version 1.0. *Eur J Nucl Med Mol Imaging*. 2019;46:540–557.
12. Malkowski B, Harat M, Zyromska A, et al. The sum of tumour-to-brain ratios improves the accuracy of diagnosing gliomas using ^{18}F-FET PET. *PLos One*. 2015;10:e0140917.
13. Rapp M, Heinzel A, Galldiks N, et al. Diagnostic performance of ^{18}F-FET PET in newly diagnosed cerebral lesions suggestive of glioma. *J Nucl Med*. 2013;54:229–235.
14. Thon N, Kunz M, Lemke L, et al. Dynamic ^{18}F-FET PET in suspected WHO grade II gliomas defines distinct biological subgroups with different clinical courses. *Int J Cancer*. 2015;136:2132–2145.
15. Sun A, Liu X, Tang G. Carbon-11 and fluorine-18 labeled amino acid tracers for positron emission tomography imaging of tumors. *Front Chem*. 2017; 5:124.
16. Shoup TM, Olson J, Hoffman JM, et al. Synthesis and evaluation of [18F]1-amino-3-fluorocyclobutane-1-carboxylic acid to image brain tumors. *J Nucl Med*. 1999;40:331–338.
17. Schuster DM, Savir-Baruch B, Nieh PT, et al. Detection of recurrent prostate carcinoma with anti-1-amino-3-18F-fluorocyclobutane-1-carboxylic acid PET/CT and ^{111}In-capromab pendetide SPECT/CT. *Radiology*. 2011;259: 852–861.
18. Schuster DM, Votaw JR, Nieh PT, et al. Initial experience with the radiotracer anti-1-amino-3-18F-fluorocyclobutane-1-carboxylic acid with PET/CT in prostate carcinoma. *J Nucl Med*. 2007;48:56–63.
19. Sorensen J, Owenius R, Lax M, et al. Regional distribution and kinetics of [18F]fluciclovine (anti-[18F]FACBC), a tracer of amino acid transport, in subjects with primary prostate cancer. *Eur J Nucl Med Mol Imaging*. 2013; 40:394–402.
20. Wakabayashi T, Iuchi T, Tsuyuguchi N, et al. Diagnostic performance and safety of positron emission tomography using ^{18}F-fluciclovine in patients with clinically suspected high- or low-grade gliomas: a multicenter phase IIb trial. *Asia Ocean J Nucl Med Biol*. 2017;5:10–21.
21. Kondo A, Ishii H, Aoki S, et al. Phase IIa clinical study of [^{18}F]fluciclovine: efficacy and safety of a new PET tracer for brain tumors. *Ann Nucl Med*. 2016;30:608–618.
22. Akhurst T, Beattie B, Gogiberidze G, et al. [18F]FACBC Imaging of recurrent gliomas: a comparison with [11C]methionine and MRI. *J Nucl Med*. 2006;47: 79P.
23. Bogsrud T, Loendalen A, Brandal P, et al. ^{18}F-fluciclovine (FACBC) PET/CT in residual or recurrent gliomas. *J Nucl Med*. 2016;57:1512.
24. Tsuyuguchi N, Terakawa Y, Uda T, et al. Diagnosis of brain tumors using amino acid transport PET imaging with ^{18}F-fluciclovine: a comparative study with L-methyl-^{11}C-methionine PET imaging. *Asia Ocean J Nucl Med Biol*. 2017;5:85–94.
25. Wang L, Qu W, Lieberman BP, et al. Synthesis, uptake mechanism characterization and biological evaluation of F-18 labeled fluoroalkyl phenylalanine analogs as potential PET imaging agents. *Nucl Med Biol*. 2011;38:53–62.
26. Galldiks N, Stoffels G, Ruge MI, et al. Role of O-(2-18F-fluoroethyl)-L-tyrosine PET as a diagnostic tool for detection of malignant progression in patients with low-grade glioma. *J Nucl Med*. 2013;54:2046–2054.
27. Jansen NL, Graute V, Armbruster L, et al. MRI-suspected low-grade glioma: is there a need to perform dynamic FET PET? *Eur J Nucl Med Mol Imaging*. 2012;39:1021–1029.
28. Jansen NL, Suchorska B, Wenter V, et al. Prognostic significance of dynamic ^{18}F-FET PET in newly diagnosed astrocytic high-grade glioma. *J Nucl Med*. 2015;56:9–15.
29. la Fougere C, Suchorska B, Bartenstein P, et al. Molecular imaging of gliomas with PET: opportunities and limitations. *Neuro Oncol*. 2011;13: 806–819.
30. Popperl G, Kreth FW, Herms J, et al. Analysis of ^{18}F-FET PET for grading of recurrent gliomas: is evaluation of uptake kinetics superior to standard methods? *J Nucl Med*. 2006;47:393–403.
31. Huang C, McConathy J. Radiolabeled amino acids for oncologic imaging. *J Nucl Med*. 2013;54:1007–1010.
32. Ellingson BM, Bendszus M, Boxerman J, et al. Consensus recommendations for a standardized Brain Tumor Imaging Protocol in clinical trials. *Neuro Oncol*. 2015;17:1188–1198.
33. Unsgard G, Solheim O, Lindseth F, et al. Intra-operative imaging with 3D ultrasound in neurosurgery. *Acta Neurochir Suppl*. 2011;109:181–186.
34. Karlberg A, Berntsen EM, Johansen H, et al. Multimodal ^{18}F-Fluciclovine PET/MRI and ultrasound-guided neurosurgery of an anaplastic oligodendroglioma. *World Neurosurg*. 2017;108:989.e1–989.e8.
35. Rivaz H, Chen SJ, Collins DL. Automatic deformable MR-ultrasound registration for image-guided neurosurgery. *IEEE Trans Med Imaging*. 2015;34: 366–380.
36. Floeth FW, Pauleit D, Sabel M, et al. Prognostic value of O-(2-18F-fluoroethyl)-L-tyrosine PET and MRI in low-grade glioma. *J Nucl Med*. 2007;48:519–527.
37. Kracht LW, Miletic H, Busch S, et al. Delineation of brain tumor extent with [11C]L-methionine positron emission tomography: local comparison with stereotactic histopathology. *Clin Cancer Res*. 2004;10: 7163–7170.
38. Pafundi DH, Laack NN, Youland RS, et al. Biopsy validation of ^{18}F-DOPA PET and biodistribution in gliomas for neurosurgical planning and radiotherapy target delineation: results of a prospective pilot study. *Neuro Oncol*. 2013;15:1058–1067.
39. Pauleit D, Floeth F, Hamacher K, et al. O-(2-[18F]fluoroethyl)-L-tyrosine PET combined with MRI improves the diagnostic assessment of cerebral gliomas. *Brain*. 2005;128:678–687.
40. Heiss P, Mayer S, Herz M, et al. Investigation of transport mechanism and uptake kinetics of O-(2-[18F]fluoroethyl)-L-tyrosine in vitro and in vivo. *J Nucl Med*. 1999;40:1367–1373.
41. Habermeier A, Graf J, Sandhofer BF, et al. System L amino acid transporter LAT1 accumulates O-(2-fluoroethyl)-L-tyrosine (FET). *Amino Acids*. 2015; 47:335–344.
42. Kim DK, Kim IJ, Hwang S, et al. System L-amino acid transporters are differently expressed in rat astrocyte and C6 glioma cells. *Neurosci Res*. 2004; 50:437–446.
43. Oka S, Okudaira H, Ono M, et al. Differences in transport mechanisms of trans-1-amino-3-[18F]fluorocyclobutanecarboxylic acid in inflammation, prostate cancer, and glioma cells: comparison with L-[methyl-11C] methionine and 2-deoxy-2-[18F]fluoro-D-glucose. *Mol Imaging Biol*. 2014; 16:322–329.

44. Oka S, Okudaira H, Yoshida Y, et al. Transport mechanisms of trans-1-amino-3-fluoro[1-(14)C]cyclobutanecarboxylic acid in prostate cancer cells. *Nucl Med Biol*. 2012;39:109–119.
45. Okudaira H, Nakanishi T, Oka S, et al. Kinetic analyses of trans-1-amino-3-[18F]fluorocyclobutanecarboxylic acid transport in Xenopus laevis oocytes expressing human ASCT2 and SNAT2. *Nucl Med Biol*. 2013;40:670–675.
46. Fuchs BC, Bode BP. Amino acid transporters ASCT2 and LAT1 in cancer: partners in crime? *Semin Cancer Biol*. 2005;15:254–266.
47. Kaira K, Oriuchi N, Imai H, et al. l-type amino acid transporter 1 and CD98 expression in primary and metastatic sites of human neoplasms. *Cancer Sci*. 2008;99:2380–2386.
48. Nakanishi T, Tamai I. Solute carrier transporters as targets for drug delivery and pharmacological intervention for chemotherapy. *J Pharm Sci*. 2011;100: 3731–3750.
49. Sidoryk M, Matyja E, Dybel A, et al. Increased expression of a glutamine transporter SNAT3 is a marker of malignant gliomas. *Neuroreport*. 2004; 15:575–578.
50. Unterrainer M, Schweisthal F, Suchorska B, et al. Serial ^{18}F-FET PET imaging of primarily ^{18}F-FET-negative glioma: does it make sense? *J Nucl Med*. 2016;57:1177–1182.
51. Villanueva-Meyer JE, Mabray MC, Cha S. Current clinical brain tumor imaging. *Neurosurgery*. 2017;81:397–415.
52. Arita H, Yamasaki K, Matsushita Y, et al. A combination of TERT promoter mutation and MGMT methylation status predicts clinically relevant subgroups of newly diagnosed glioblastomas. *Acta Neuropathol Commun*. 2016;4:79.
53. Xiao Y, Eikenes L, Reinertsen I, et al. Nonlinear deformation of tractography in ultrasound-guided low-grade gliomas resection. *Int J Comput Assist Radiol Surg*. 2018;13:457–467.